The J domain of Tpr2 regulates its interaction with the proapoptotic and cell-cycle checkpoint protein, Rad9

著者	Xiang Shuang-Lin, Iwasaki Shu-ichi, Kumano Tomoyasu, Sun Xiangao, Yoshioka Katsuji, Yamamoto Ken-ichi, 善岡 克次
journal or publication title	Biochemical and Biophysical Research Communications
volume	287
number	4
page range	932-940
year	2001-10-01
URL	http://hdl.handle.net/2297/1794

The J domain of Tpr2 regulates its interaction with the proapoptotic and cell-cycle checkpoint protein, Rad9

Shuang-Lin Xiang*, Tomoyasu Kumano*¶, Shu-ichi Iwasaki*, Xiangao Sun*, Kastuji Yoshioka*#, and Ken-chi Yamamoto*#§

*Department of Molecular Pathology and #Center for the Development of Molecular Target Drugs, Cancer Research Institute, Kanazawa University, Kanazawa 920-0934, Japan

¶Department of Radiology, Kanazawa University School of Medicine, Kanazawa University, Kanazawa 920-0934, Japan

§To whom correspondence should be addressed: Department of Molecular Pathology, Cancer Research Institute, Kanazawa University, 13-1 Takaramachi, Kanazawa 920-0934, Japan; Phone, 81-76-265-2755; Fax, 81-76-234-4516; E-mail, kyamamot@kenroku.kanazawa-u.ac.jp;

Abbreviations used in this paper: DMEM, Dulbecco's modified Eagle medium; FCS, fetal calf serum; GST, glutathione S-transferase; IB, immunoblot; IP, immunoprecipitation; JNK, c-jun N-terminal kinase; PCNA, proliferating cell nuclear antigen; PKR, dsRNA-dependent protein kinase; TNF-α, tumor necrosis factor-α; tpr, tetratricopeptide repeat; Tpr2, Tetratricopeptide repeat protein2.

Abstract

Human Rad9 is a key cell-cycle checkpoint protein that is postulated to function in the early phase of cell-cycle checkpoint control through complex formation with Rad1 and Hus1. Rad9 is also thought to be involved in controlling apoptosis through its interaction with Bcl-2. To explore the biochemical functions of Rad9 in these cellular control mechanisms, we performed two-hybrid screening and identified Tetratricopeptide repeat protein 2 (Tpr2) as a novel Rad9-binding protein. We found that Tpr2 binds not only to Rad9, but also to Rad1 and Hus1, through its N-terminal tetratricopeptide repeat region, as assessed by in vivo and in vitro binding assays. However, the in vivo and in vitro interactions of Tpr2 with Rad9 were greatly enhanced by the deletion of its C-terminal J domain or by a point mutation in the conserved HPD motif in the J domain, though the binding of Tpr2 to Rad1 and Hus1 was not influenced by these J-domain mutations. We further found; (1) Rad9 transiently dissociates from Tpr2 following heat-shock or UV treatments, but the mutation of the J domain abrogates this transient dissociation of the Tpr2/Rad9 complex; and (2) the J domain of Tpr2 modulates the cellular localization of both Tpr2 itself and Rad9. These results indicate that the J domain of Tpr2 plays a critical role in the regulation of both physical and functional interactions between Tpr2 and Rad9.

Key Words: cell cycle checkpoint, apoptosis, chaperone, tetratricopeptide repeat, J domain, Rad9, Hus1, Rad1

Introduction

Cell-cycle checkpoints are surveillance mechanisms that monitor the cell cycle and protect genome integrity by inducing cell-cycle arrest or programmed cell death (apoptosis) in response to DNA damage or DNA replication errors. Because several features of cell cycle checkpoints have been conserved throughout evolution, information about cell cycle checkpoints learned from yeast provides a framework for developing a further understanding of the checkpoint pathways in higher eukaryotes (1, 2). Genetic studies in the fission yeast *S. pombe* have identified three key checkpoint molecules ($Rad1^+$, $Hus1^+$, and $Rad9^+$) (3-5) and mammalian homologs of these molecules have been identified (6-8). These checkpoint molecules show some homology with nucleases (9, 10) and proliferating cell nuclear antigen (PCNA), and are thought to function in the early phase of the cell-cycle checkpoint pathway as a part of a checkpoint protein complex (11-13). Of these checkpoint molecules, Rad9 may have an additional unique function, because it contains a 15-amino-acid region near its N-terminus that is significantly homologous to the BH3 domains conserved among many of the apoptotic Bcl-2 family (14-16). To study the biochemical functions of mammalian Rad9 as both a checkpoint and a possible apoptotic molecule, we used a yeast two-hybrid method with full-length human Rad9 as bait, and identified Tpr2 (Tetratricopeptide repeat protein 2) as a novel Rad9-binding factor.

Tpr2 was first identified as a factor interacting with the GAP-related domain of neurofibromin in two-hybrid screening, and is a member of the growing Tpr family (17). All members of this family contain various numbers of a degenerate 34-amino-acid

repeated motif called a tetratricopeptide repeat (tpr). The tpr's are protein-protein interacting motifs, and function in diverse cellular processes such as cell-cycle control, transcription repression, stress response, protein kinase inhibition, mitochondrial and peroxisomal protein transport, and neurogenesis (18, 19). Tpr2 contains seven tpr motifs in its N-terminus and has been reported to bind Hsc70 through these tpr motifs (20). In addition, in its C-terminus, Tpr2 has a typical J domain found among members of the Hsp40/DnaJ co-chaperone family (21). The Hsp40/DnaJ family members regulate the chaperone activity of Hsp70/Hsc70 by stimulating their intrinsic ATPase activity; therefore, it is plausible that Tpr2 also functions as a co-chaperone in various cellular processes. Indeed, Tpr2, together with Hsp40, has been identified as a suppressor of polyglutamine-mediated degeneration in a *Drosophila* experimental system (22). In addition, p58, the most closely related homolog of Tpr2 in the Tpr family, has been characterized as a physiological inhibitor of dsRNA-dependent protein kinase (PKR), a primary mediator of the antiviral and antiproliferative properties of interferon (23). More recently, p58 has been shown to inhibit the apoptosis induced by PKR and the inflammatory cytokine TNF-α (24). However, the precise cellular functions of Tpr2 remain to be clarified.

In the present study, we show that Tpr2 binds not only to Rad9, but also to Rad1 and Hus1, in vivo. However, unlike the interactions of Tpr2 with Rad1 or Hus1, both the in vivo Tpr2/Rad9 interaction and the cellular localization of Rad9 are influenced by the J domain of Tpr2. These results indicate a critical role for the J-domain of Tpr2 in functional interactions between Tpr2 and Rad9. The possible physiological significance

of this finding is discussed.

Experimental Procedures

Yeast two-hybrid screening. Total RNA was isolated from MCF7 cells using TRIZOL® Reagent (GibcoBRL®) and was used for first-strand cDNA synthesis with random primers using SuperScript™ II RNase H- Reverse Transcriptase (GibcoBRL®), according to the manufacturer's instructions. The cDNA encoding the complete human Rad9 coding sequence (amino acids 1-391) (6) was then amplified by PCR with a Pfx DNA polymerase (GibcoBRL®) using the following primers: 5' sense, 5'-TTGGATCCATATGAAGTGCCTGGTCACGGGC-3'; 3' antisense, 5'-ATGGATCCCTCAGCCTTCACCCTCACTGTCT-3'. The amplified PCR products were digested with BamHI and subcloned into pAS2. Both the coding sequence of Rad9 and the junction sequences between pAS2 and Rad9 were confirmed by sequencing using the Thermo Sequenase™ II dye terminator cycle sequencing premix kit (Amersham Pharmacia Biotech). For yeast two-hybrid screening, a human lymphocyte cDNA library in pACT (Clontech) was transformed into *S. cerevisiae* CG1945 containing pAS2-Rad9, according to the user's manual. The verified positive cDNAs were sequenced, and proteins with similar sequences were sought using GenomeNet (Kyoto University, Japan).

Construction of expression plasmids. The cDNA encoding the full-length Tpr2 (17) (Tpr2/FL, Figure 1A) was amplified by PCR using BglII site-directed primers (5' sense primer, 5'-AATAAGATCTATGGCGGCGACCGAGCCGGAGCT-3'; 3' antisense

primer, 5’-CCCGGAGATCTCTTAGCCAAATTGAAAAAAGAAAT-3’). The cDNA encoding the N-terminal portion of Tpr2 (containing the tpr motifs but lacking the J domain) (Tpr2/ΔJ, Figure 1A) was isolated by two-hybrid screening as described above. These cDNAs were digested and subcloned into pFlag-CMV-2 (Kodak) at BamHI sites to generate pFlag-CMV-Tpr2/FL and pFlag-CMV-Tpr2/ΔJ. A 90-bp NcoI-SmaI fragment of pFlag-CMV-2 containing the Flag-tag coding sequence and multiple cloning sites was inserted into XbaI (filled in)-digested pEF-Bos to create a Flag-tagged expression vector, pEF-Flag. To construct Flag-tagged expression vectors encoding various Tpr2 deletion mutants (Figure 2A), the BglII-directed primers described above and the following primers were used for PCR: 3’ antisense primer (5’-ACCGGATCCATTGGTGGAATCCATTCGTA-3’) for pEF-Flag-Tpr2/5’-motif (amino acids 1-199); 5’ sense primer (5’-CTTGGATCCGCTCAGGCACAACAAGAGTT-3’) for pEF-Flag-Tpr2/3’-motif (amino acids 120-384). These cDNAs were then digested and cloned into pEF-Flag. A 129-bp XbaI fragment of KSII(+)-3xHA containing the HA-tagged sequence and multiple cloning sites was inserted into XbaI-digested pEF-Bos to create the HA-tagged expression vector, pEF-3xHA. This plasmid was then used to construct expression vectors encoding Tpr2/ΔJ (pEF-3xHA-Tpr2/ΔJ), Tpr2/FL (pEF-3xHA-Tpr2/FL), human Rad1 (8) (pEF-3xHA-Rad1) and human Hus1 (pEF-3xHA-Hus1); the human Hus1 cDNA was cloned by two hybrid screening as described above. HA-tagged expression plasmids encoding the entire Rad9 coding sequence (amino acids 1-391) and various Rad9 deletion mutants (Figure 3A) were constructed using the following primers: 5’

sense, 5’-AATGGATCCATGAAGTGCCTGGTCACGGGC-3’(starts at amino acid 1); 3’ antisense, 5’-ATGGATCCCTCAGCCTTCACCCTCACTGTCT-3’(ends at amino acid 391); 5’ sense, 5’-AATAGATCTCCCTTGGAGGACGGGCTC-3’(starts at amino acid 31); 3’ antisense, 5’-AAAGATCTGGCTTTGGCAGTGCTGTCTGCCT-3’(ends at amino acid 192); 5’ sense, 5’-ACCGGATCCATGGTGACTGAGATGTGCCTT-3’(starts at amino acid193); 5’-sense, 5’-AATGGATCCTCCCTGCAGGCCGTCTTCGAC-3’ (starts at amino acid 131).

Site-directed mutagenesis was performed using a two-round PCR method. In the first set of reactions, the partial 5’ and 3’ fragments of the Tpr2HPD mutant (Figure 1A) were amplified with the BglII site-directed outside primers (5’ sense, 5’-AATAAGATCTATGGCGGCGACCGAGCCGGAGCT-3’; 3’antisense, 5’-CCCGGAGATCTCTTAGCCAAATTGAAAAAAGAAAT-3’) and the overlapping inside primers encoding the H399Q mutation (underlined in the primers) (5’-sense, 5’-GCCTTGATGCACCA<u>A</u>CCAGATCGGCATAGT-3’; 3’ antisense, 5’-TCCACTATGCCGATCTGG<u>T</u>TGGTGCATCAA-3’). The PCR products were purified and mixed in equimolar concentrations, then used as templates for the second round of PCR amplification with the outside primers described above, and finally subcloned into pEF-Flag and pEF-3xHA expression vectors. Sequence analysis confirmed that there were no unintentional PCR-introduced mutations. The expression vector encoding HA-tagged JNK1 (pEF-3xHA-JNK1) was described previously (25).

Co-immunoprecipitation and immunoblotting. Cos7 cells were grown in

Dulbecco's Modified Eagle's Medium (DMEM, Gibco-BRL, Life Technologies) supplemented with 10% heat inactivated fetal calf serum (FCS, Gibco-BRL), 50 units/ml of penicillin G and 50 μg/ml streptomycin sulfate (Gibco-BRL) in a 5% CO_2 humidified incubator. The cells were transiently transfected with 15 μg of various expression vectors as indicated in the Figures, using the DEAE-dextran method. At 36 hrs after transfection, cells were harvested, spun down and lysed in 0.5 ml of lysis buffer [50 mM HEPES (pH 7.5), 150 mM NaCl, 1% NP-40, 10% glycerol, 2 mM $MgCl_2$, 1 mM EGTA, 20 mM β-glycerophosphate, 2 mM Na_3VO_4, 1 mM phenylmethylsulfonyl fluoride, 0.2 mM dithiothreitol]. The debris was then discarded after centrifugation at 12,000 rpm for 15 min at 4˚C. The whole-cell lysate was assayed for protein quantity, using a Bio-Rad protein assay kit. For co-immunoprecipitation, 1 μl of mouse anti-Flag M5 antibodies at 3.4 μg/μl (Sigma) was added to 1.5 mg of cell lysate, and the mixtures were then rotated for 2 hrs at 4˚C; then 20 μl of a 50% slurry of Protein G-sepharose beads was added and the mixtures were rotated for 2 more hrs at 4˚C. The beads were washed with lysis buffer four times, then resuspended in SDS sample buffer and boiled 5 min. Mouse anti-Flag M5, rat high-affinity anti-HA (Boehringer Mannheim), or rabbit anti-human Rad9 antibodies were used as the first antibodies for western blotting at a 1:2000 dilution; Horse anti-mouse IgG (H&L [heavy and light chains]) HRP-linked (New England Biolabs), goat anti-rat IgG (H&L) HRP-linked (Funakoshi), or goat anti-rabbit IgG (H&L) HRP-linked (Funakoshi) antibodies were used as second antibodies at a 1:4000 dilution. Rabbit anti-human Rad9 antibody was kindly provided by S. P. Jackson (The WellcomeCRC Institute, University

of Cambridge).

In vitro protein binding assay. The complete Rad9 (amino acids 1-391), Rad1 (amino acids 1-282) and Hus1 (amino acids 1-280) cDNAs were subcloned into the BlueScript vector for in vitro translation. To generate glutathione-S-transferase (GST)-Tpr2 fusion proteins, the cDNA encoding Tpr2/FL (amino acids 1-484) or the Tpr2/ΔJ fragment (amino acids 1-384) was subcloned into pGEX-4T-3 (Amersham Pharmacia Biotech). GST fusion proteins were induced with 0.2 mM isopropyl-beta-D-thiogalactopyranoside (Sigma) and purified from host *E. coli* XL1-Blue at 30˚C using glutathione-conjugated agarose beads (Amersham Pharmacia Biotech). Rad9, Rad1 and Hus1 were transcribed and translated in vitro in the presence of [^{35}S]-methionine using Rabbit Reticulocyte Lysate (Promega) according to the manufacturer's instructions. Ten micrograms of GST, GST-Tpr2/FL, or GST-Tpr2/ΔJ attached to glutathione-conjugated agarose beads were mixed with 25 μl of the lysate containing translated proteins in binding buffer (50 mM HEPES/KOH, pH 7.5, 100 mM KOAc, 5 mM $Mg(OAc)_2$, 5 mM DTT, 10% glycerol, 1% NP-40, 1 mM phenylmethylsulfonyl fluoride). After 1 hr of rotation at room temperature, the beads were recovered and washed, then resuspended in SDS sample buffer and fractioned by SDS-PAGE followed by autoradiography.

Immunofluorescence. To establishMCF-7 cell lines that stably express Flag-tagged full-length Tpr2 or HPD mutant Tpr2 proteins, linearized plasmids (pSV2-neo and pFlag-CMV2-Tpr2/FL or pEF-Flag-Tpr2/HPD mutant, at the molar ratio of 1 to 20) were transfected into MCF-7 cells (25 μg of DNA/5x10^6 cells) by electroporation (220

mV, 960 μF). After two weeks of G418 (400 μg/ml, Nacalai Tesque) selection, G418-resistant clones were analyzed for Tpr2 protein expression. The parental MCF-7 cells and stable transfectant lines were plated on cover slips and grown to 30% confluence. They were then transiently transfected with pEF-3xHA-Rad9 using DOSPER liposomal transfection reagents (Roche). Twenty hours after transfection, the cells were washed twice with PBS, fixed in 3% paraformaldehyde/PBS, and permeabilized by 0.1% NP-40/PBS for 20 minutes. Cells were blocked for 40 minutes in 1% bovine serum albumin in PBS containing 0.1% Tween-20, and incubated 2 hrs with rat high-affinity anti-HA or mouse anti-Flag M5 antibodies in blocking buffer. Finally, immune complexes were stained with Rhodamine-conjugated anti-Rat IgG or FITC-conjugated anti-Mouse IgG antibodies. Stained cells were analyzed using a Zeiss LSM510 laser-scanning confocal microscope.

Results

Identification of Tpr2 as a Rad9-binding factor by two-hybrid screening

Using a pACT-packaged human lymphocyte cDNA library and the entire human Rad9 coding sequence in pAS2 as bait, we sequentially screened approximately 1 x 10^7 cotransformants of *S. cerevisiae* CG1945 for proteins that directly interact with Rad9. Of 90 His+ clones, 47 LacZ+ clones were chosen for further study. After plasmid rescue, these clones were digested by EcoRI and XhoI and sorted into four groups. Bait-dependent binding was confirmed within two of the groups: one large group containing 40 clones and another containing 4 clones. Within each group, at least two

clones were randomly selected for sequence analysis and protein homology search. We found that the insert in the large group encoded Hus1 and the insert in the small group encoded Tpr2. Although the interaction of human Rad9 with human Hus1 was demonstrated previously (26-28), the interaction of Rad9 with Tpr2 had not been reported.

The Tpr2 cDNA that we isolated from the two-hybrid screening did not contain the entire Tpr2 coding sequence; rather, it contained the sequence from nucleotide 7 to nucleotide 1753 of the full-length Tpr2 cDNA (17). Furthermore, the nucleotide sequence 1149-1408 was deleted, thus generating a new stop codon, with the deduced amino acid sequence stopping at amino acid 384 (Fig. 1A). We named this protein Tpr2/ΔJ, because it does not contain the C-terminal J domain but still contains all seven of the N-terminal tpr motifs. Because there were no typical GU·····AG conserved sequences near the deleted portion of the Tpr2 cDNA, and because we could not detect Tpr2/ΔJ expression in many different types of cell lines (data not shown), it is unlikely that Tpr2/ΔJ is a splicing variant of Tpr2.

The J domain of Tpr2 modulates interactions with Rad9 but not with Hus1 and Rad1

To confirm that Tpr2 binds to Rad9 in vivo as well as in vitro, we performed co-immunoprecipitation and GST pull-down experiments. Because Rad9 can form stable complexes with Hus1 and Rad1 (13, 26-28), these binding analyses were also performed for Hus1 and Rad1. For the in vivo binding experiments, we transiently cotransfected Cos7 cells with HA-tagged expression vectors encoding Rad9, Hus1, or

Rad1 with Flag-tagged expression vectors encoding either Tpr2/ΔJ or Tpr2/FL (Fig. 1A). As shown in Figure 1B and 1C, immunoprecipitation of Tpr2/ΔJ or Tpr2/FL with an anti-Flag (M5) antibody brought down, not only the HA-tagged Rad9, but also the HA-tagged Hus1 and Rad1, indicating that the N-terminal tpr region of Tpr2 binds these proteins. However, the Tpr2/ΔJ protein, lacking the J domain, showed much stronger binding to Rad9 than did the full-length Tpr2 protein (Tpr2/FL) (compare lane 2 in Fig. 1B and Fig. 1C). Furthermore, the binding patterns of Tpr2/ΔJ and Tpr2/FL with Hus1 or Rad1 were similar, indicating that the J domain influences only the interaction between Tpr2 and Rad9.

To further study the effect of the J domain on the Tpr2/Rad9 interaction, we introduced a point mutation in the conserved HPD motif of the Tpr2 J-domain (HPD mutant, Figure 1A). As shown in Figure 1D, the HPD mutant of Tpr2 also showed very strong binding to Rad9 (actually stronger than that of Tpr2/ΔJ). These results indicate that, while the N-terminal tpr region of Tpr2 are binding sites for Rad9, the J domain plays a critical role in the interaction between Rad9 and Tpr2 in vivo. Consistent with these in vivo results, in vitro binding analysis showed that GST-Tpr2/ΔJ also bound to the Rad9 protein translated in vitro by rabbit reticulocyte lysates more effectively than did GST-Tpr2/FL (Figure 1E, lanes 3 and 5). We further found that GST-Tpr2/ΔJ and GST-Tpr2/FL bound similarly to Rad1 and Hus1 (data not shown), again supporting a specific role for the J domain in the Tpr2/Rad9 interaction. In addition, the inclusion of ATP in the Mg^{2+}-containing binding buffer inhibited the binding of Rad9 to GST-Tpr2/FL, but not to GST-Tpr2/ΔJ (Figure 1E, lanes 3-6). Because J domains

function as co-chaperones for chaperones such as Hsp70, which utilize ATP hydrolysis for their function (21), the results of these binding experiments suggest that the Tpr2/Rad9 interaction is regulated by the Tpr2-J-domain's co-chaperone activity, presumably together with major chaperones such as Hsp70.

Binding site mapping for the Tpr2/Rad9 interaction

The results shown in Figures 1 indicated that the N-terminal tpr region of Tpr2 were the primary binding sites for Rad9. Tpr2 contains seven tpr motifs; therefore, we constructed expression vectors encoding the N-terminal and C-terminal parts of these tpr motifs (Figure 2A) to further define the binding sites in Tpr2 for Rad9, Hus1, and Rad1 as well as for Tpr2 itself. Expression vectors encoding these tpr motif mutants were transfected into Cos7 cells and the binding activity of these mutants for Rad9, Hus1, Rad1, and Tpr2 was examined by co-immunoprecipitation experiments. As shown in Figure 2B, the 5'-motif of Tpr2 (amino acids 1-199), containing the three N-terminal tpr motifs, is sufficient to support binding to Rad9. While these N-terminal tpr motifs of Tpr2 appeared to be important for Rad1 binding as well, both the N-terminal and C-terminal tpr motifs and even the J domain appeared to be required for Hus1 binding and Tpr2 homodimerization (Figure 2B).

Rad9 contains three functional regions (Figure 3A): (1) the N-terminal BH3-like region, which may have proapoptotic functions similar to the BH3 domains conserved in Bcl-2 family members (15); (2) the 3' to 5'exonuclease (3' to 5')-like region, which may be involved in DNA damage repair (10); and (3) the C-terminal Rad1- and Hus1-binding region (28). To define the binding sites for Tpr2 in Rad9, expression vectors

encoding various parts of Rad9 (Figure 3A) were transfected and co-immunoprecipitation experiments were carried out. The results shown in Figure 3B indicate several unique features of Rad9. Firstly, Rad9 was mainly phosphorylated in its C-terminal Rad1/Hus1 binding region (lanes 2-5). Secondly, the N-terminal BH3-like region was dispensable for Tpr2 binding, but its deletion enhanced the binding of Rad9 to the wild-type Tpr2 (lanes 11 and 12). Finally, both of the non-overlapping N-terminal (amino acids 1-192, 3'-del) and C-terminal (amino acids 193-391, C-terminal) regions of Rad9 bound to Tpr2 (lanes 2 and 4). However, while the wild-type (FL) and HPD mutant Tpr2 bound equally to the N-terminal region of Rad9 (amino acids 1-192, 3'-del) (lanes 4 and 10), the C-terminal regions of Rad9 (amino acids 131-391, 5'-del; amino acids 193-391, C-terminal) could only bind to the HPD mutant of Tpr2 (lanes 2, 3, 8, and 9).

Functional links between Rad9 and Tpr2

Because Hsp70 was implicated as a possible cofactor in the J-domain-dependent interaction between Tpr2 and Rad9 (Figure 1E) and because it is a major heat-inducible protein, we hypothesized that heat-shock treatment would modulate the interaction between Tpr2 and Rad9. To test this hypothesis, Cos7 cells were cotransfected with HA-tagged Rad9 expression vectors and Flag-tagged expression vectors encoding the wild-type (FL) and HPD mutant of Tpr2, and subjected to heat shock treatment (at 43˚C for 60 minutes). Tpr2/Rad9 binding was then analyzed by co-immunoprecipitation. As shown in Figure 4, while the HPD mutant of Tpr2 continued to bind strongly to Rad9 after heat-shock treatment (lanes 6-10), Rad9 became transiently dissociated from the

wild-type Tpr2 (lanes 1-5). These results indicate that the Rad9/Tpr2 interaction is modulated in cellular responses to stress, such as heat-shock, in a J-domain-dependent manner.

To study further possible functional links between Rad9 and Tpr2, we established MCF-7 cell lines that stably expressed the wild-type (FL) and HPD mutant of Tpr2. The parental MCF-7 cells and stable cell lines were transiently transfected with HA-tagged Rad9 expression vectors and the cellular localization of transiently expressed Rad9 as well as of stably expressed the wild-type and HPD mutant of Tpr2 was then analyzed by immuno-fluorescence confocal microscopy. Previous studies disagreed about the exact cellular location of Rad9. Two studies showed Rad9 to be exclusively localized to the nucleus (27, 29), whereas a third study showed Rad9 to be located throughout the cell, but concentrated in the nucleus and partially overlapping with Bcl-2 on the intracellular membranes (15). As shown in Figure 5 (upper panels), we observed Rad9 to be almost exclusively localized to the nucleus in parental MCF-7 cells. However, in MCF-7 cells stably over-expressing Tpr2/FL, Rad9 was located in the cytoplasm as well as in the nucleus and was co-localized with Tpr2/FL in these cellular compartments (middle panels, Figure 5). Interestingly, the HPD mutant of Tpr2 was mainly localized to the nucleus, and Rad9 in these cells was again co-localized with the HPD mutant of Tpr2, mainly in the nucleus (lower panels, Figure 5). These results indicate that the J domain of Tpr2 modulates the cellular localization, not only of Tpr2 itself, but also of Rad9.

Discussion

In an attempt to further characterize Rad9 functions in cell-cycle checkpoint as well as apoptotic control, we identified Tpr2 as a novel Rad9-binding protein. The results of in vitro GST pulldown and co-immunoprecipitation assays indicated that Tpr2 binds, not only to Rad9, but also to other Rad9 partners such as Rad1 and Hus1, through its N-terminal tpr motifs. However, deletion of the C-terminal J domain of Tpr2 or a point mutation in the conserved HPD motif in the J domain strongly enhanced the in vivo interaction of Tpr2 with Rad9, but not with Rad1 or Hus1 (Figure 1), indicating that the interaction between Tpr2 and Rad9 is regulated by the J domain of Tpr2. In vitro binding experiments further showed that ATP inhibits the binding of Tpr2 to Rad9 (Figure 1E). The J domains of the Hsp40/DnaJ family are known to regulate the chaperone activity of Hsp70/Hsc70 through stimulation of their intrinsic ATPase activity (21), and Tpr2 has been shown to bind to Hsc70 through its N-terminal tpr motifs (20). These findings suggest that Tpr2 acts as a co-chaperone for the Hsc70/Hsp70 chaperones.

Rad9 contains two Tpr2-binding sites. While the in-vivo interaction of Tpr2 with the N-terminal part of Rad9 is not influenced by the Tpr2's J domain, the interaction of Tpr2 with the C-terminal part of Rad9, which is mainly phosphorylated in vivo, is very strongly enhanced by a point mutation in the conserved HPD motif in the J domain (Figure 3B). This raises an interesting possibility that Rad9 phosphorylation plays an important role in the interaction between Rad9 and Tpr2. However, it is unlikely that Rad9 phosphorylation itself is critical for the J domain-dependent interaction between

Tpr2 and Rad9, because the in vitro translated and unphosphorylated C-terminal region of Rad9 also showed an enhanced binding to the Tpr2 protein lacking the J domain (unpublished data). Further work is required to define precise functional roles for these two non-overlapping Tpr2-binding regions of Rad9 in the interaction between Rad9 and Tpr2.

To explore possible functional interactions between Tpr2 and Rad9, we studied Rad9 localization in MCF-7 cells that overexpressed either wild-type Tpr2 or Tpr2 with a point mutation in the conserved HPD motif. We found Rad9 to be almost exclusively localized in the nucleus of parental MCF-7 cells. However, Rad9 was located in both the cytoplasm and nucleus in MCF-7 cells that stably over-expressed the wild-type Tpr2, and was co-localized with Tpr2 in these cellular compartments. Interestingly, the point mutation in the HPD motif resulted in the redistribution of Tpr2 mainly to the nucleus, and Rad9 was again co-localized with the HPD mutant of Tpr2, mainly in the nucleus (Figure 5). We also studied the in vivo Tpr2/Rad9 interaction after treatment with noxious stimuli such as heat-shock (Figure 4) or UV radiation (data not shown). We found that, while Rad9 transiently dissociated from Tpr2 following these treatments, the HPD mutation abolished this transient dissociation of the Tpr2/Rad9 complex. These results therefore indicated that the J domain of Tpr2 plays a critical role in the regulation of both the cellular localization of Tpr2 and Rad9 and the complex formation between them.

Here we presented evidence for physical and functional interactions between Tpr2 and Rad9 and for their regulation by the J domain of Tpr2. Although genetically

identified as one of key molecules acting in the early phase of cell-cycle checkpoint control, the precise biochemical functions of Rad9 remain to be established. Because Rad9, Rad1 and Hus1 show a structural similarity to PCNA (11-13) and because these three molecules, whether derived from *S. pombe* (13) or human (26-28), form a tri-molecular complex, it has been postulated recently that they function as a PCNA-like, DNA-sliding clamp complex, coupling DNA repair and DNA synthesis to cell cycle checkpoint control (11-13). In addition, recent studies showed that human and *S. pombe* Rad9 contains a BH3-like sequence in its N terminus that is conserved among members of the Bcl-2 apoptotic family and that Rad9 interacts with Bcl-2 through this BH3 motif (15, 16). Furthermore, over-expression of the Rad9 gene from either organism in human cells can cause apoptosis in a BH3-motif-dependent manner (15). On the other hand, the physiological functions of Tpr2 are not clear, although Tpr2 has structural properties characteristic of co-chaperones (17, 22). To explore further possible physiological implications, we studied the effects of wild-type or mutant Tpr2 over-expression on the interactions of Rad9 with Rad1 or Hus1, but have not observed any significant effects so far (unpublished data). However, while cells that stably over-expressed wild-type Tpr2 were more resistant to the apoptosis induced by UV radiation or heat-shock, cells that over-expressed Tpr2 containing a point mutation in the conserved HPD motif in the J domain showed enhanced spontaneous apoptosis as well as enhanced apoptosis induced by UV radiation or heat-shock (unpublished data). This observation suggests that Tpr2 modulates stress-induced apoptosis through its interaction with Rad9. Since recent studies have shown that Hsp70 negatively regulates several steps in apoptotic

pathways that are initiated by diverse stimuli (30-33), it is further possible that Tpr2 functions to co-operate with Hsp70/Hsc70 in this apoptotic regulation. Further work is required to define the observed effects of Tpr2 on apoptosis.

Acknowledgements

We thank S. P. Jackson and R. Freire for discussion as well as providing human Rad1 cDNA and an anti-Rad9 antibody, and K. Nagata and M. Mori for discussion. This work was supported in part by a Grant-in-aid from the Ministry of Education, Science and Culture of Japan.

References:

1 O'Connell, M. J., Walworth, N. C. and Carr, A. M. (2000) The G2-phase DNA-damage checkpoint. *Trends Cell Biol.* **10,** 296-303

2 Zhou, B. S. and Elledge, S. J. (2000) The DNA damage response:putting checkpoints in perspective. *Nature* **408,** 433-439

3 Al-Khodairy, F. and Carr, A. M. (1992) DNA repair mutants defining G2 checkpoint pathways in *Schizosaccharomyces pombe*. *EMBO J.* **11,** 1343-1350

4 Enoch, T., Carr, A. M. and Nurse, P. (1992) Fission yeast genes involved in coupling mitosis to completion of DNA replication. *Genes Dev.* **6,** 2035-2046

5 Rowley, R., Subramani, S. and Young, P. G. (1992) Checkpoint controls in *Schizosaccharomyces pombe: rad1*. *EMBO J.* **11,** 1335-1342

6 Lieberman, H. B., Hopkins, K. M., Nass, M., Demetrick, D. and Davey, S.

(1996) A human homolog of the Schizosaccharomyces pombe rad9+ checkpoint control gene. *Proc. Natl. Acad. Sci. USA* **93,** 13890-13895

7 Kostrub, C. F., Knudsen, K., Subramani, S. and Enoch, T. (1998) Hus1p, a conserved fission yeast checkpoint protein, interacts with Rad1p and is phosphorylated in response to DNA damage. *The EMBO Journal* **17,** 2055-2066

8 Freire, R., Murguia, J. R., Tarsounas, M., Lowndes, N. F., Moens, P. B. and Jackson, S. P. (1998) Human and mouse homologs of Schizosaccharomyces pombe rad1+ and Saccharomyces cerevisiae RAD17: linkage to checkpoint control and mammalian meiosis. *Genes Dev.* **12,** 2560-2573

9 Parker, A. E., Weyer, I. V. d., Laus, M. C., Oostveen, I., Yon, J., Verhasselt, P. and Luyten, W. H. M. L. (1998) A human homologue of the Schizosaccharomyces pombe rad1+ checkpoint gene encodes an exonuclease. *J. Biol. Chem.* **273,** 18332-18339

10 Bessho, T. and Sancar, A. (2000) Human DNA damage checkpoint protein hRAD9 is a 3' to 5' exonuclease. *J. Biol. Chem.* **275,** 7451-7454

11 Thelen, M. P., Venclovas, C. and Fidelis, K. (1999) A sliding clamp model for the Rad1 family of cell cycle checkpoint proteins. *Cell* **96,** 769-770

12 Venclovas, C. and Thelen, M. P. (2000) Structure-based predictions of Rad1, Rad9, Hus1 and Rad17 participation in sliding clamp and clamp-loading complexes. *Nucl. Acids Res.* **28,** 2481-2493

13 Caspari, T., Dahlen, M., Kanter-Smoler, G., Lindsay, H. D., Hofmann, K., Papadimitriou, K., Sunnerhagen, P. and Carr, A. M. (2000) Characterzation of

Schizosaccharomyces pombe Hus1: a PCNA-related protein that associates with Rad1 and Rad9. *Mol. Cell. Biol.* **74,** 1254-1262

14 Huang, D. C. S. and Strasser, A. (2000) BH3-only proteins-essntial initators of apoptotic cell death. *Cell* **103,** 839-842

15 Komatsu, K., Miyashita, T., Hang, H., Hopkins, K. M., Zheng, W., Cuddeback, S., Yamada, M., Lieberman, H. B. and Wang, H.-G. (2000) Human homologue of S.pombe Rad9 interacts with BCL-2/BCL-xl and promotes apoptosis. *Nature Cell Biol.* **2,** 1-6

16 Komatsu, K., Hopkins, K. M., Lieberman, H. B. and Wang, H.-G. (2000) Schizosaccharomyces pombe Rad9 contains a BH3-like region and interacts with the anti-apoptotic protein Bcl-2. *FEBS Letters* **481,** 122-126

17 Murthy, A. E., Bernards, A., Church, D., Wasmuth, J. and Gusella, J. F. (1996) Identification and characterization od two novel tetratricopeptide repeat-containing genes. *DNA Cell Biol.* **15,** 727-735

18 Goebl, M. and Yanagida, M. (1991) The TPR snap helix: a novel protein repeat motif from mitosis to transcription. *TIBS* **16,** 173-177

19 Lamb, J. R., Tugendreich, S. and Hieter, P. (1995) Tetratrico peptide repeat interactions: to TPR or not to TPR? *TIBS* **20,** 257-259

20 Liu, F.-H., Wu, S.-J., Hu, S.-M., Hsiao, C.-D. and Wang, C. (1999) Specific interaction of the 70-kDa heat shock cognate protein with the tetratricopeptide repeats. *J. Biol. Chem.* **274,** 34425-34432

21 Kelley, W. L. (1998) The J-domain family and the recruitment of chaperone

power. *TIBS* **23,** 222-227

22 Kazemi-Esfarjani, P. and Benzer, S. (2000) Genetic Suppression of polyglutamine toxicity in Drosophila. *Science* **287,** 1837-1840

23 Lee, T. G., Tang, N., Thompson, S., Miller, J. and Katze, M. G. (1994) The 58,000-Dalton cellular inhibitor of the interferon-induced double-stranded RNA-activated protein kinase (PKR) is a member of the tetratricopeptide repeat family of proteins. *Mol. Cell. Biol.* **14,** 2331-2342

24 Tang, N. M., Korth, M. J., Jr., M. G., Wambach, M., Der, S. D., Bandyopadhyay, S. K., Williams, B. R. G. and Katze, M. G. (1999) Inhibition of double-stranded RNA- and tumor necrosis factor Alpha-mediated apoptosis by tetratricopeptide repeat protein and cochaperone p58IPK. *Mol. Cell. Biol.* **19,** 4757-4765

25 Ito, M., Yoshioka, K., Akechi, M., Yamashita, S., Takamatsu, N., Sugiyama, K., Hibi, M., Nakabeppu, Y., Shiba, T. and Yamamoto, K. (1999) JSAP1, a novel JNK3-binding proteinthat functions as a scaffold factor in the JNK signaling pathway. *Mol. Cell. Biol.* **19,** 7539-7548

26 Volkmer, E. and Karnitz, L. M. (1999) Human homologs of Schizosaccharomyces pombe Rad1, Hus1 and Rad9 form a DNA damage-responsive protein complex. *J. Biol. Chem.* **274,** 567-570

27 Onge, R. P. S., Udell, C. M., Casselman, R. and Davey, S. (1999) The human G2 checkpoint control protein hRad9 is a nuclear phosphoprotein that forms complexes with hRad1 and hHus1. *Mol. Cell. Biol.* **10,** 1985-1995

28 Hang, H. and Lieberman, H. B. (2000) Physical interactions among human

checkpoint control proteins Hus1p, Rad1p and Rad9p and implications for the regulation of cell cycle progression. *Genomics* **65,** 24-33

29 Burtelow, M. A., Kaufmann, S. H. and Karnitz, L. M. (2000) Retention of the hRad9 checkpoint complex in extraction-resistant nuclear complexes after DNA damage. *J. Biol. Chem.* **275,** 26343-26348

30 Beere, H. M., Wolf, B. B., Cain, K., Mosser, D. D., Mahboubi, A., Kuwana, T., Tailor, P., Morimoto, R. I., Cohen, G. M. and Green, D. R. (2000) Heat-shock protein 70 inhibits apoptosis by preventing recruitment of procaspase-9 to the Apaf-1 apoptosome. *Nature Cell Biol.* **2,** 469-475

31 Saleh, A., Srinivasula, S. M., Balkir, L., Robbins, P. D. and Alnemri, E. S. (2000) Negative regulation of the Apsf-1 apoptosome by Hsp70. *Nature Cell Biol.* **2,** 476-483

32 Mosser, D. D., Caron, A. W., Bourget, L., Meriin, A. B., Y.Sherman, M., Morimoto, R. I. and Massie, B. (2000) The chaperone function of hsp70 is required for protection against stress-induced apoptosis. *Mol. Cell. Biol.* **20,** 7146-7159

33 Gabai, V. L., Yaglom, J. A., Volloch, V., MeriiN, A. B., Force, T., Koutroumanis, M., Massie, B., Mosser, D. D. and Sherman, M. Y. (2000) Hsp72-mediated suppression of c-jun N-terminal kinase is implicated in development of tolerance to caspase-independent cell death. *Mol. Cell. Biol.* **20,** 6826-6836

Figure Legends

Figure 1 Tpr2 binds to Rad9 in vivo and in vitro.

(A) Schematic diagram of Tpr2 and its mutants. Tpr2 contains seven tpr motifs and the J domain, as indicated. (B, C) Cos7 cells at 40% confluence in 10-cm dishes were transiently co-transfected with 15 μg of pFlag-CMV2-Tpr2/ΔJ (B) or pFlag-CMV2-Tpr2/FL (C) and 15 μg of pEF-3xHA-Rad9 (lanes 2, 6, and 10), pEF-3xHA-Hus1 (lanes 3, 7, and 11), or pEF-3xHA-Rad1 (lanes 4, 8, and 12), as indicated; pEF-3xHA-JNK1 (lanes 1, 5, and 9) was used as a control. Thirty-six hours after transfection, cellular lysates were immunoprecipitated with anti-Flag antibodies, and the immunoprecipitates were subjected to immunoblot analysis using anti-HA antibodies (IP, lanes 1-4). To check protein expression levels, 10% of the cellular lysates were directly subjected to immunoblot analysis (IB) using either anti-HA antibodies (lanes 5-8) or anti-Flag antibodies (lanes 9-12). Rad9, Hus1, Rad1, and JNK1 are indicated by the star. (D) Flag-tagged expression vectors encoding wild-type Tpr2 (FL: lanes 1, 4, and 7), the HPD mutant of Tpr2 (lanes 2, 5, and 8), or JNK1 (lanes 3, 6, and 9) were cotransfected with HA-tagged Rad9 expression vectors. Cellular lysates were immunoprecipitated with anti-Flag antibodies, followed by immunoblot analysis using anti-HA antibodies (IP, lanes 1-3). Protein expression levels were checked by immunoblotting (IB) with anti-HA (lanes 4-6) or anti-Flag (lanes 7-9) antibodies. (E) Rad9 was translated in vitro using rabbit reticulocyte lysates in the presence of [^{35}S]-methionine. Translated proteins were incubated with either GST (lanes 1 and 2), GST-Tpr2/ΔJ (lanes 3 and 4), or GST-Tpr2/FL (lanes 5 and 6) proteins attached to

glutathione-conjugated agarose beads in the absence or presence of 5 mM ATP, as indicated.

Figure 2 Binding analysis of Tpr2 deletion mutants.

(A) Schematic diagram of Tpr2 and various truncated mutants of Tpr2 used for the in-vivo binding assay. (B) Flag-tagged expression vectors encoding various Tpr2 mutants were cotransfected with HA-tagged expression vectors encoding Rad9, Rad1, Hus1, or Tpr2, as indicated. Co-immunoprecipitation was carried out with anti-Flag antibodies, followed by immunoblot analysis with anti-Rad9 or anti-HA antibodies (IP). Protein levels were checked by immunoblot analysis (IB).

Figure 3 Binding analysis of Rad9 deletion mutants.

(A) Schematic diagram of Rad9 and various truncated mutants of Rad9 used for the in vivo binding assay. (B) HA-tagged expression vectors encoding various Rad9 deletion mutants were cotransfected with Flag-tagged expression vectors encoding either the HPD mutant (lanes 2-6) or wild-type (FL, lanes 8-12) Tpr2, as indicated. HA-tagged JNK1 expression vectors were used as the negative control (lanes 1 and 7). The upper panel shows the results of the co-immunoprecipitation (IP). The middle and lower panels (immunoblot, IB) show the protein expression levels of Rad9, Tpr2, and JNK1.

Figure 4 Rad9 transiently dissociates from Tpr2 after heat-shock.

Thirty-six hours after cotransfection with Rad9 expression vectors and expression vectors encoding the wild-type (FL, lanes 1-5) or HPD mutant (lanes 6-10) Tpr2, Cos7 cells were exposed to heat-shock treatment (at 43˚C for 60 min). Following treatment, fresh medium was added for extended incubation as indicated and cellular lysates were

prepared for co-immunoprecipitation experiments (IP, upper panel). The middle and the lower panels (immunoblot, IB) show the protein expression levels of Rad9 and Tpr2, respectively.

Figure 5 The J domain-dependent colocalization of Rad9 and Tpr2.

MCF-7 cells (upper panel) and transfectants that stably expressed either Flag-Tpr2/FL (middle panel) or the Flag-Tpr2/HPD mutant (lower panel) were transiently transfected with HA-Rad9 expression vectors. Twenty hours after transfection, cells were reacted with anti-Flag or anti-HA antibodies, followed by staining with Rhodamine (Rad9, red)- or FITC (Tpr2, green)-conjugated secondary antibodies, and finally analyzed by fluorescence confocal microscopy.

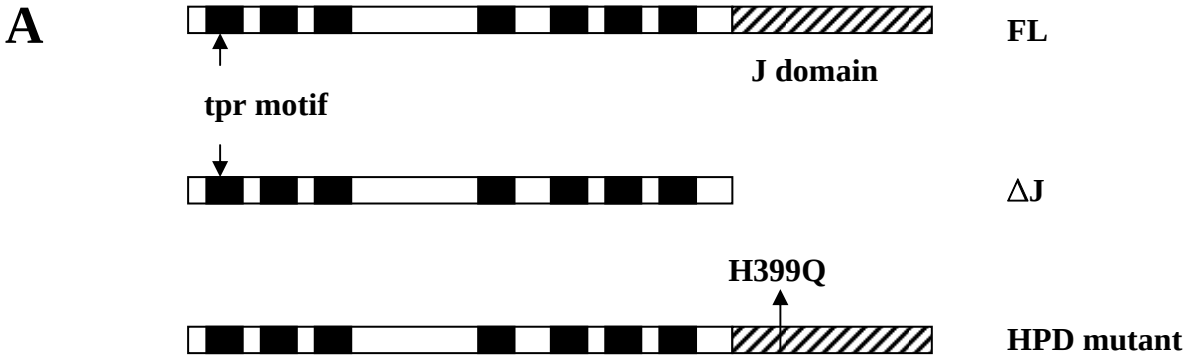
A
FL
J domain
tpr motif
ΔJ
H399Q
HPD mutant

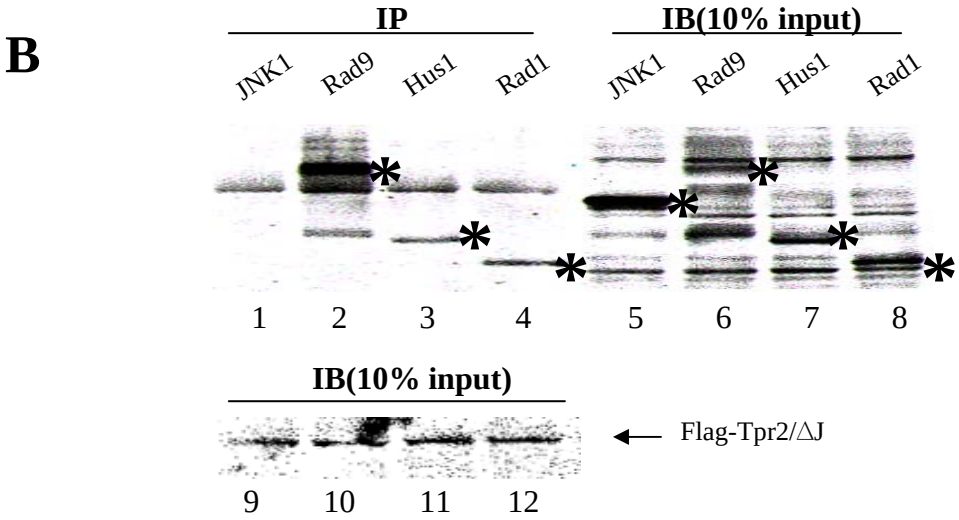
B
IP
IB(10% input)
JNK1
Rad9
Hus1
Rad1
JNK1
Rad9
Hus1
Rad1
1 2 3 4 5 6 7 8
IB(10% input)
Flag-Tpr2/ΔJ
9 10 11 12

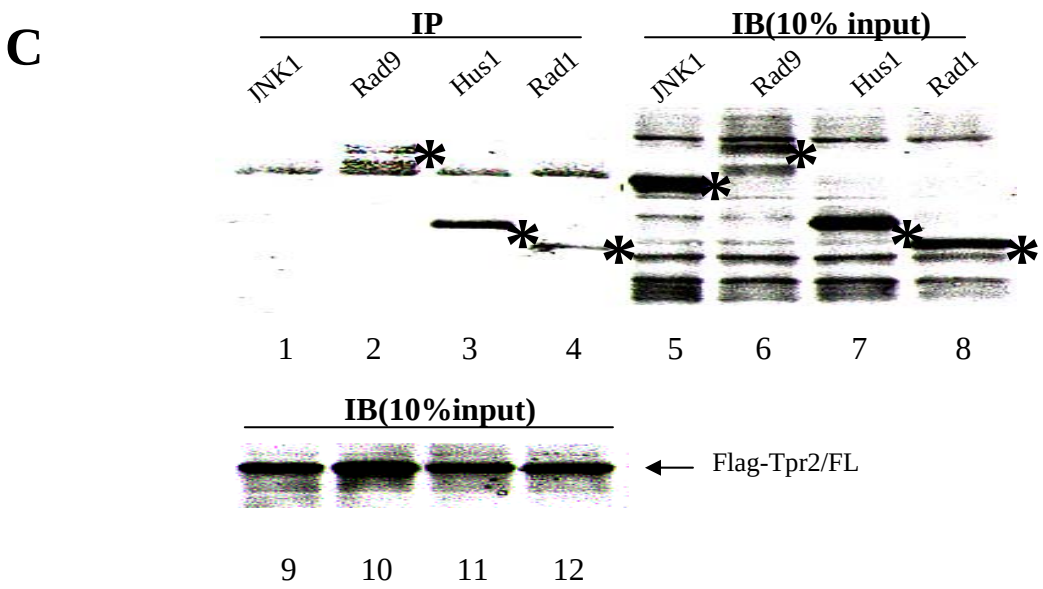
C
IP
IB(10% input)
JNK1
Rad9
Hus1
Rad1
JNK1
Rad9
Hus1
Rad1
1 2 3 4 5 6 7 8
IB(10%input)
Flag-Tpr2/FL
9 10 11 12

Fig.1A-C

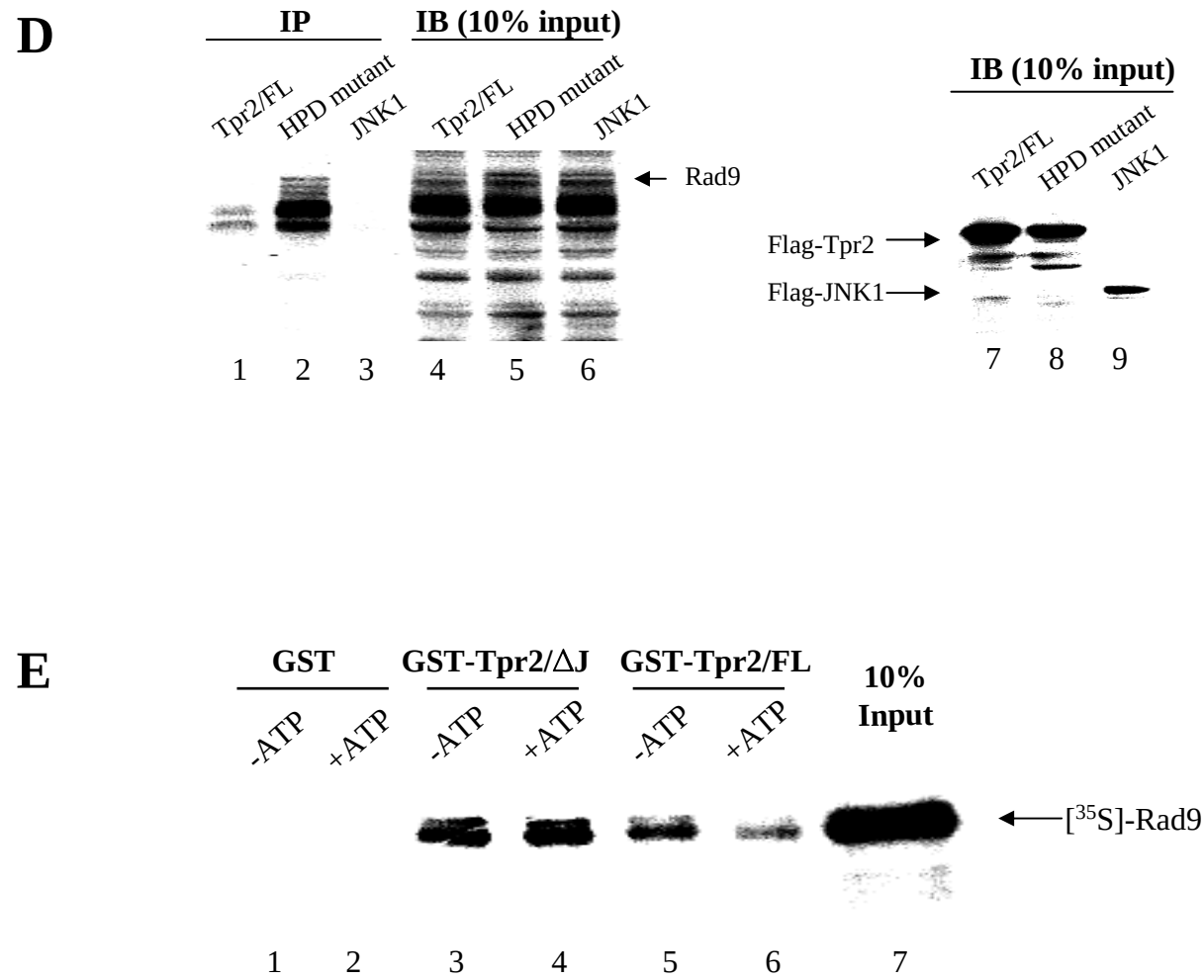
D
IP
IB (10% input)
Tpr2/FL
HPD mutant
JNK1
Tpr2/FL
HPD mutant
JNK1
Rad9
IB (10% input)
Tpr2/FL
HPD mutant
JNK1
Flag-Tpr2
Flag-JNK1
1 2 3 4 5 6 7 8 9
E
GST
GST-Tpr2/ΔJ
GST-Tpr2/FL
10% Input
-ATP
+ATP
-ATP
+ATP
-ATP
+ATP
[35S]-Rad9
1 2 3 4 5 6 7

Fig.1D-E

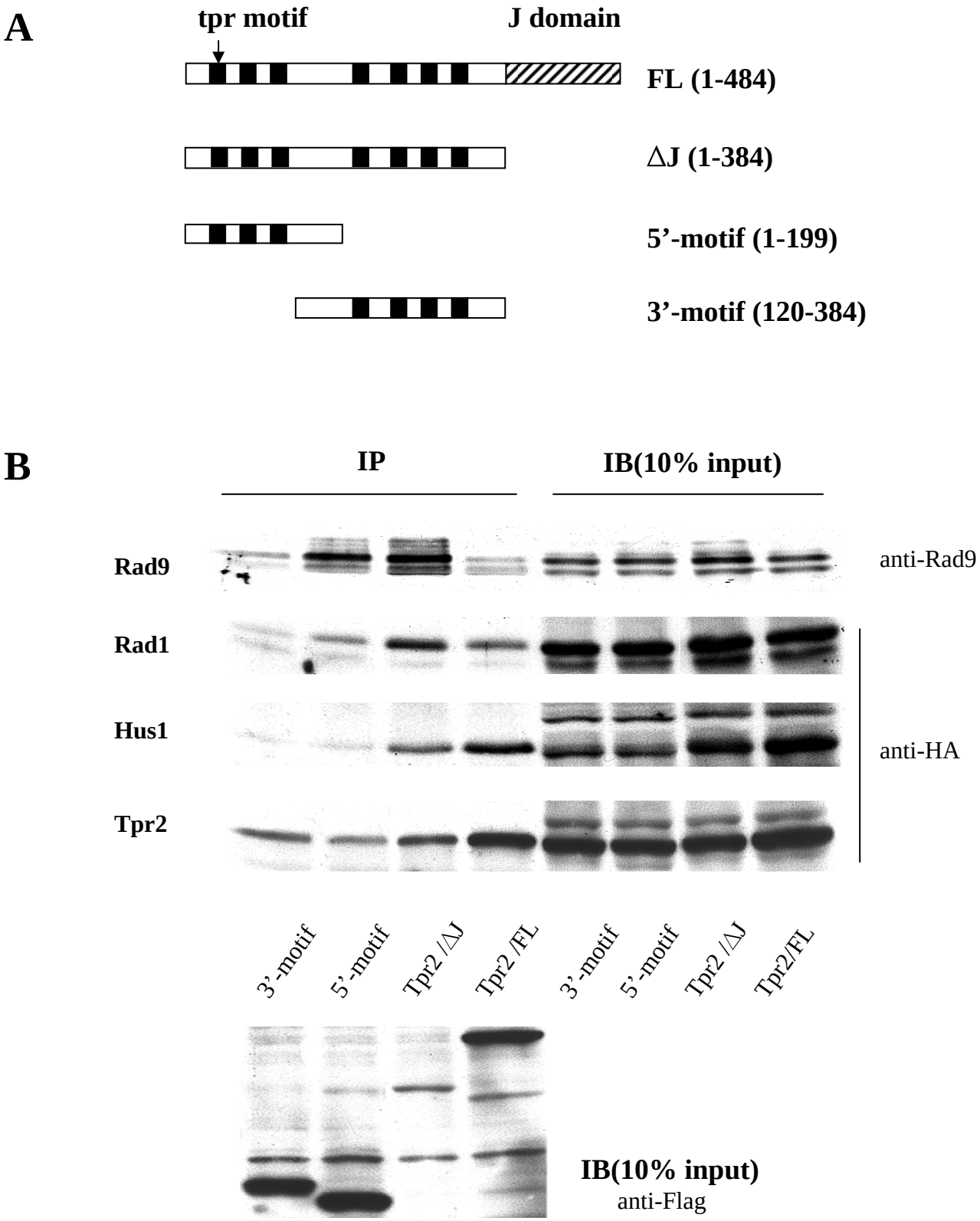
A
tpr motif
J domain
FL (1-484)
ΔJ (1-384)
5'-motif (1-199)
3'-motif (120-384)
B
IP
IB(10% input)
Rad9
Rad1
Hus1
Tpr2
anti-Rad9
anti-HA
3'-motif
5'-motif
Tpr2 /ΔJ
Tpr2 /FL
3'-motif
5'-motif
Tpr2 /ΔJ
Tpr2/FL
IB(10% input)
anti-Flag

Fig.2

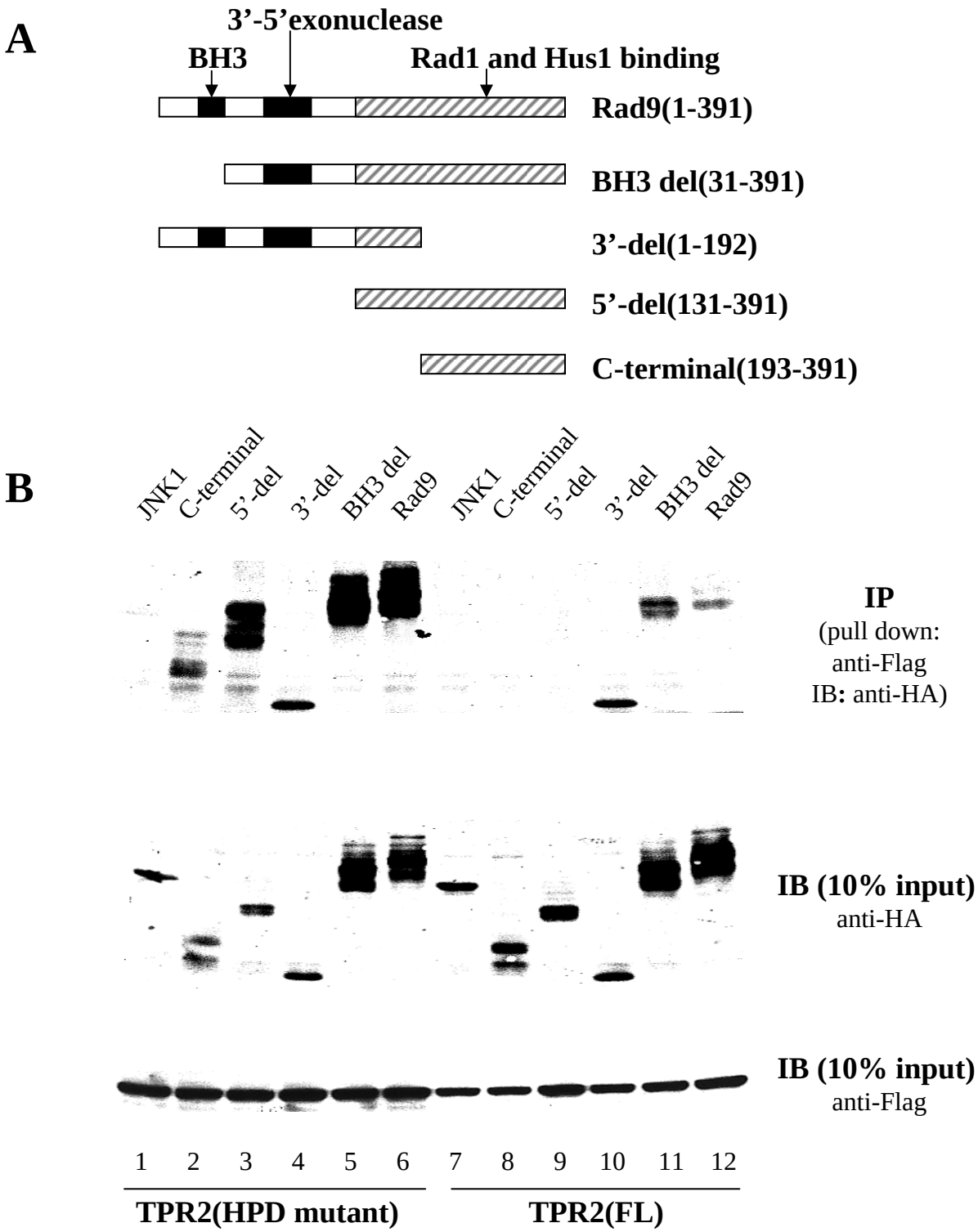
A
3'-5'exonuclease
BH3
Rad1 and Hus1 binding
Rad9(1-391)
BH3 del(31-391)
3'-del(1-192)
5'-del(131-391)
C-terminal(193-391)
B
JNK1
C-terminal
5'-del
3'-del
BH3 del
Rad9
JNK1
C-terminal
5'-del
3'-del
BH3 del
Rad9
IP
(pull down:
anti-Flag
IB: anti-HA)
IB (10% input)
anti-HA
IB (10% input)
anti-Flag
1 2 3 4 5 6 7 8 9 10 11 12
TPR2(HPD mutant)
TPR2(FL)

Fig.3

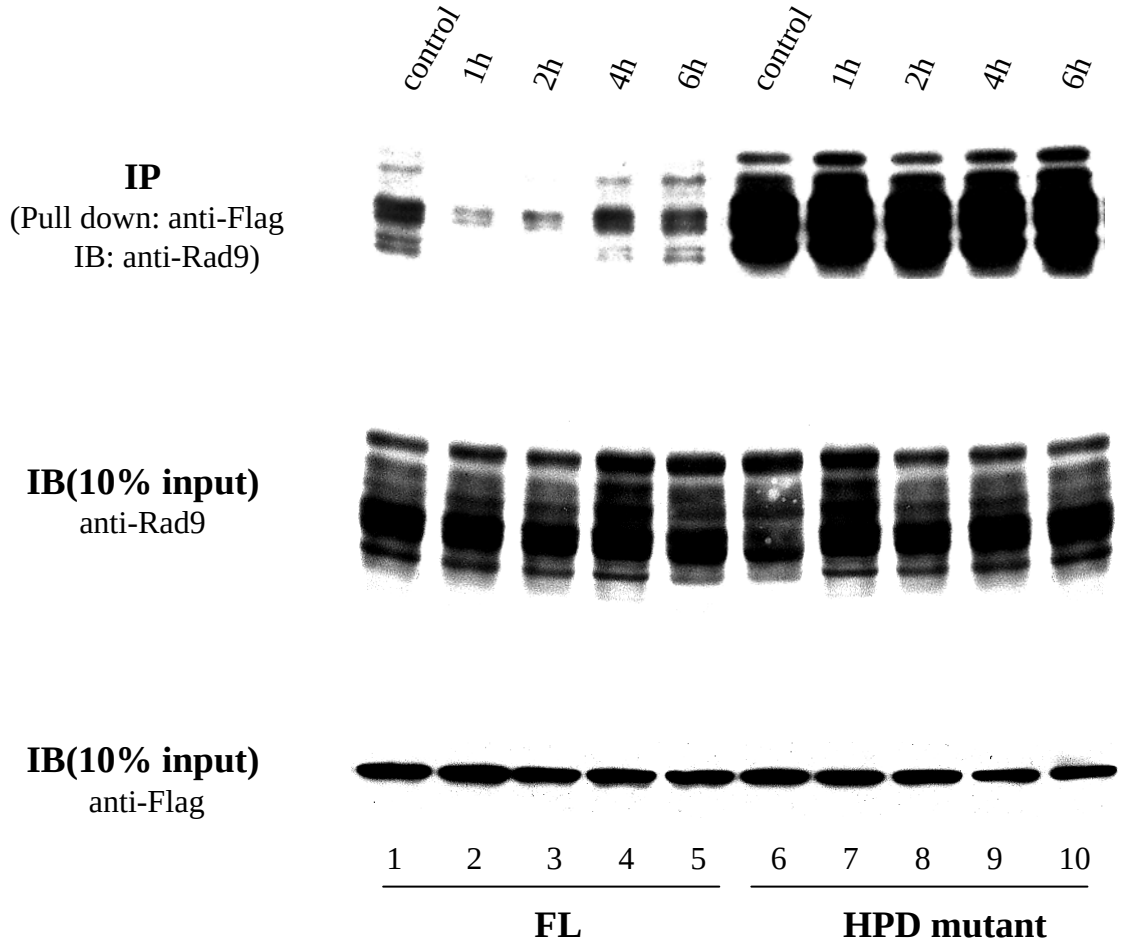
control
1h
2h
4h
6h
control
1h
2h
4h
6h
IP
(Pull down: anti-Flag
IB: anti-Rad9)
IB(10% input)
anti-Rad9
IB(10% input)
anti-Flag
1 2 3 4 5 6 7 8 9 10
FL
HPD mutant

Fig.4

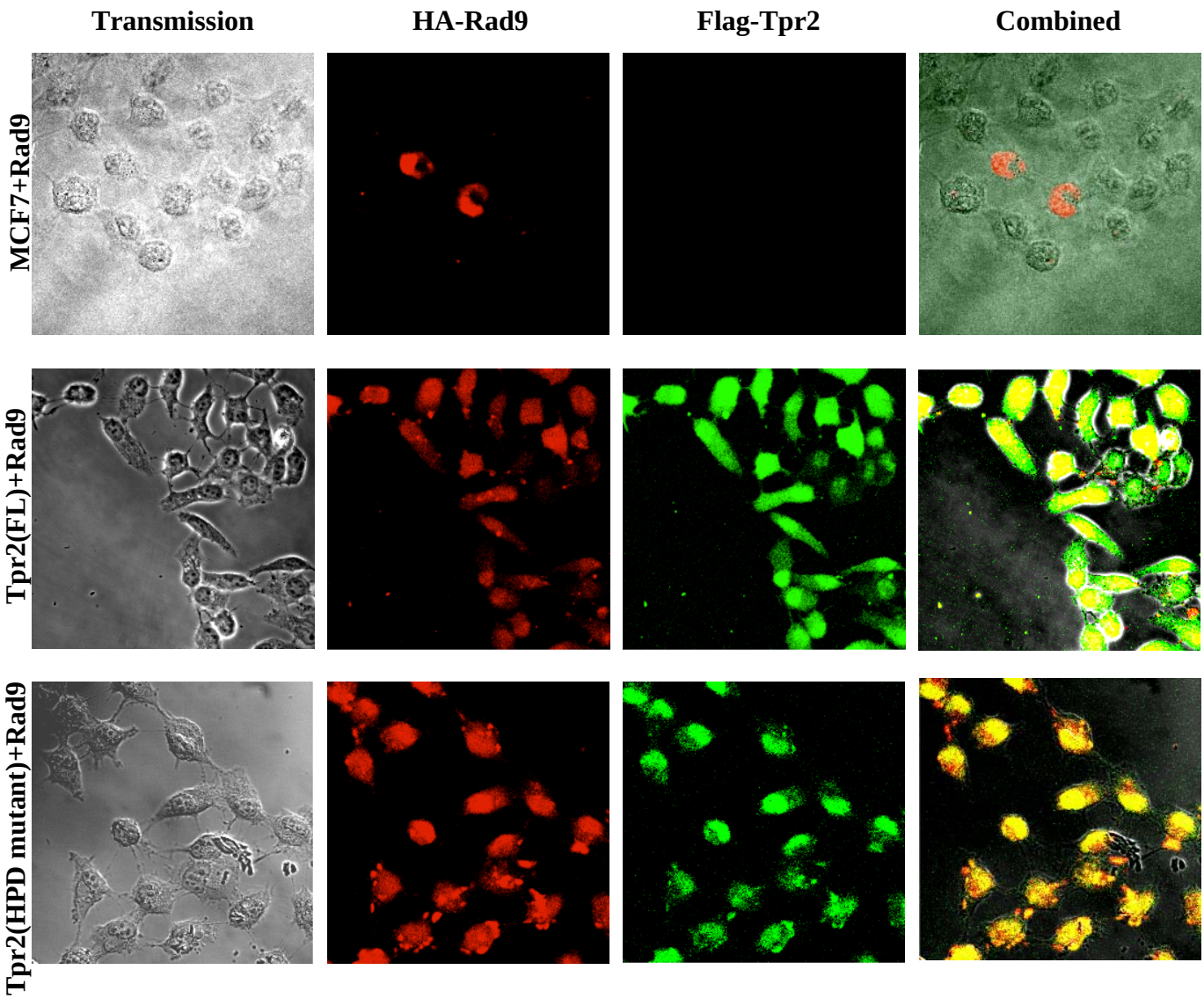
Transmission
HA-Rad9
Flag-Tpr2
Combined
MCF7+Rad9
Tpr2(FL)+Rad9
Tpr2(HPD mutant)+Rad9

Fig.5